physica status solidi a
www.pss-a.com

Check for updates

Formation Dynamics of BH and GaH-Pairs in Crystalline Silicon During Dark Annealing

*Yanik Acker, Jochen Simon, and Axel Herguth**

In crystalline silicon, atomic hydrogen released from hydrogen dimers forms acceptor–hydrogen pairs during annealing in the dark at elevated temperatures. In this study, the formation of boron–hydrogen (BH) and gallium–hydrogen (GaH) pairs in 1 Ω cm silicon is investigated at temperatures ranging from 140 to 220 °C. Acceptor–hydrogen concentrations in the low 10^{14} cm^{-3} range are quantified by means of highly sensitive resistance measurements. GaH pairs are generally found to form faster than BH pairs. Arrhenius analysis shows a difference in activation energy (BH: 1.20 eV, GaH: 1.04 eV) while the trial frequency is the same (≈4×10^8 s^{-1}).

1. Introduction

Hydrogen plays a major role not only in passivation[1–6] but also in the formation of recombination active defect complexes in crystalline silicon[7–10] and can lead to a change in device behavior over time. Upon closer inspection, atomic hydrogen may assume different charge states ($H^{+/0/-}$) depending on the Fermi-level (determined by doping, injection, and temperature) with H^+ being the dominant species in *p*-type silicon.[11] Driven by charge and its generally high diffusivity, hydrogen exhibits a complex reaction scheme in silicon[12,13] involving many different potential binding partners. Among those are dopants like boron B^- and gallium Ga^-, both negatively charged as *p*-type dopants in silicon, forming overall electrically neutral dopant-hydrogen complexes like B^-H^+ and Ga^-H^+.[14–16] This pair formation from neutral hydrogen dimers H_2,[17–20] or more precisely the splitting of the dimer $H_2 + 2\,h^+ \rightleftharpoons 2\,H^+$, following, for example, the overall reaction $H_2 + 2\,B^- + 2\,h^+ \rightleftharpoons 2\,B^-H^+$, consumes holes h^+. The resulting change in hole concentration $p(t)$ with time is detectable as a change of resistivity/conductivity and has been used in various forms since the 1980s to detect and quantify hydrogen and its reaction with acceptors in mainly, but not exclusively boron-doped silicon.[14–16,21–24]

Within this contribution, the formation of GaH pairs during dark annealing in dependence of annealing temperature is investigated by means of highly sensitive resistance measurements[25] and compared to the formation of BH pairs.

2. Experimental Section

A set of samples was prepared from boron-doped float-zone silicon (doping 1.7×10^{16} cm^{-3}, thickness 250 μm) and gallium-doped Czochralski-grown silicon (doping 1.86×10^{16} cm^{-3}, final thickness 140 μm), where the first was already chemically polished and oxide-finished while the latter required saw-damage etching in KOH (20%, 80 °C) and subsequent cleaning (Piranha solution: H_2O_2:H_2SO_4 = 1:3, 80 °C; short HF dip, 2%). All samples were coated on both sides with a 118 ± 1 nm thick hydrogen-rich silicon nitride SiN_x:H layer via plasma enhanced chemical vapor deposition (reactive gases: SiH_4 : NH_3 = 1 : 1, carrier gas: N_2, 400 °C; PlasmaLab 100 from Oxford Instruments). The samples were subjected to a rapid thermal annealing step in a belt furnace (c.FIRE 9600 from Centrotherm International AG) with a measured peak temperature of 750 ± 10 °C during which atomic hydrogen is released from the SiN_x : H layer and diffuses into the silicon substrate.[26] As a consequence of the fast cool-down ramp and rapidly decreasing solubility, atomic hydrogen predominantly forms dimers (H_{2A}),[19,20] whereby it also already comes to some extent to the formation of dopant-hydrogen pairs.[27]

For resistance measurements (described elsewhere in detail[25]), four stripe-like aluminum terminals were deposited onto the 50 mm × 50 mm samples by thermal evaporation. Electrical contact to the substrate was established by local alloying via laser heating (laser-fired contacts, LFCs).[28] The schematic sample design is shown in **Figure 1**.

To trigger the formation (and dissociation) of BH and GaH pairs, the samples were annealed on a hotplate (Praezitherm *PZ-28*, absolute uncertainty ±0.5 °C by PT100, heat/cool cycle variation ±0.5 °C) in the dark. Note that BH and GaH pairs could dissociate under illumination depending on the resulting injection. For all samples except the 160 °C BH sample, the annealing treatment was interrupted from time to time for resistance measurements on a temperature-controlled sample stage (25.0 ± 0.1 °C) in a four-terminal configuration using a 6.5 digit multimeter (Keithley 2000 Series). Resistance changes of the 160 °C BH sample were tracked in-situ on the hotplate. As

Y. Acker, J. Simon, A. Herguth
Department of Physics
University of Konstanz
78457 Konstanz, Germany
E-mail: axel.herguth@uni-konstanz.de

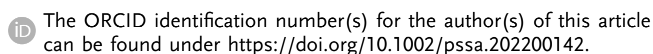
The ORCID identification number(s) for the author(s) of this article can be found under https://doi.org/10.1002/pssa.202200142.

© 2022 The Authors. physica status solidi (a) applications and materials science published by Wiley-VCH GmbH. This is an open access article under the terms of the Creative Commons Attribution-NonCommercial-NoDerivs License, which permits use and distribution in any medium, provided the original work is properly cited, the use is non-commercial and no modifications or adaptations are made.

DOI: 10.1002/pssa.202200142

 © 2022 The Authors. physica status solidi (a) applications and materials science published by Wiley-VCH GmbH

Konstanzer Online-Publikations-System (KOPS)
URL: http://nbn-resolving.de/urn:nbn:de:bsz:352-2-5m15ian72bm4

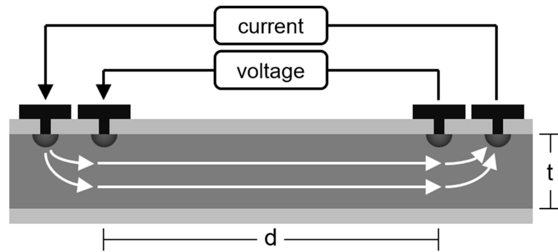

Figure 1. Sample schematic, not to scale. Locally alloyed aluminum terminals on a silicon substrate with a both-sided SiN_x : H layer. Thickness t is 250 μm (FZ-Si:B) or 140 μm (Cz-Si:Ga), inner terminal distance d is 40 mm. Resistance measurements are done in a four-terminal configuration.

discussed elsewhere in detail,[25] hole concentration p present at a certain time t can be concluded from measured resistivity ρ according to $\rho^{-1} = q \times \mu_p \times p$ (valid for p-type material) using hole mobility μ_p data from PV-Lighthouse.[29] Note that hole concentration is expected to differ from dopant concentration due to the formation of dopant-hydrogen pairs, e.g., $p = [B] - [BH]$, but that absolute quantification requires not only knowledge of the dopant concentration with an accuracy better than the expected changes by pair formation, in our case better than 0.1%, but also exact knowledge of pair concentration at a certain reference time t_0. Especially without the latter information, it is only possible to determine changes in pair concentration $\Delta[BH]$ (or $\Delta[GaH]$) from changes in hole concentration Δp where dopant concentration cancels out, i.e., $\Delta p(t, t_0) = p_t - p_{t_0} = -([BH]_t - [BH]_{t_0}) = -\Delta[BH]$ (or $\Delta p = -\Delta[GaH]$). However, one should note as well that this interpretation is valid only under the assumption that hole concentration does not change by other phenomena, e.g., formation of thermal donors. As presented elsewhere,[30] the validity of this assumption is backed up by Fourier transform infrared (FTIR) measurements at least for boron-doped samples indicating that the observed loss and gain in hole concentration coincides with the appearance and subsequent disappearance of a BH-specific absorption band.

3. Results

The observed (negative) change in hole concentration Δp with respect to the starting value during annealing in the dark at various temperatures is displayed in **Figure 2**.

3.1. Boron–Hydrogen Dynamics

In the temperature range investigated here, boron–hydrogen pairs not only form but also dissociate again, likely due to the overall cascade reaction[19,20]

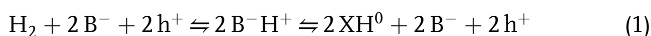

$$H_2 + 2\,B^- + 2\,h^+ \leftrightharpoons 2\,B^-H^+ \leftrightharpoons 2\,XH^0 + 2\,B^- + 2\,h^+ \tag{1}$$

where holes are consumed in the first partial reaction, but released again in the second slower partial reaction leading to the observed decrease and increase in hole concentration. XH^0 represents a neutral hydrogen complex (which might be the so far not detected H_{2C} dimer predicted by Voronkov et al.[20]) as atomic hydrogen would predominantly remain as H^+ without releasing the hole h^+

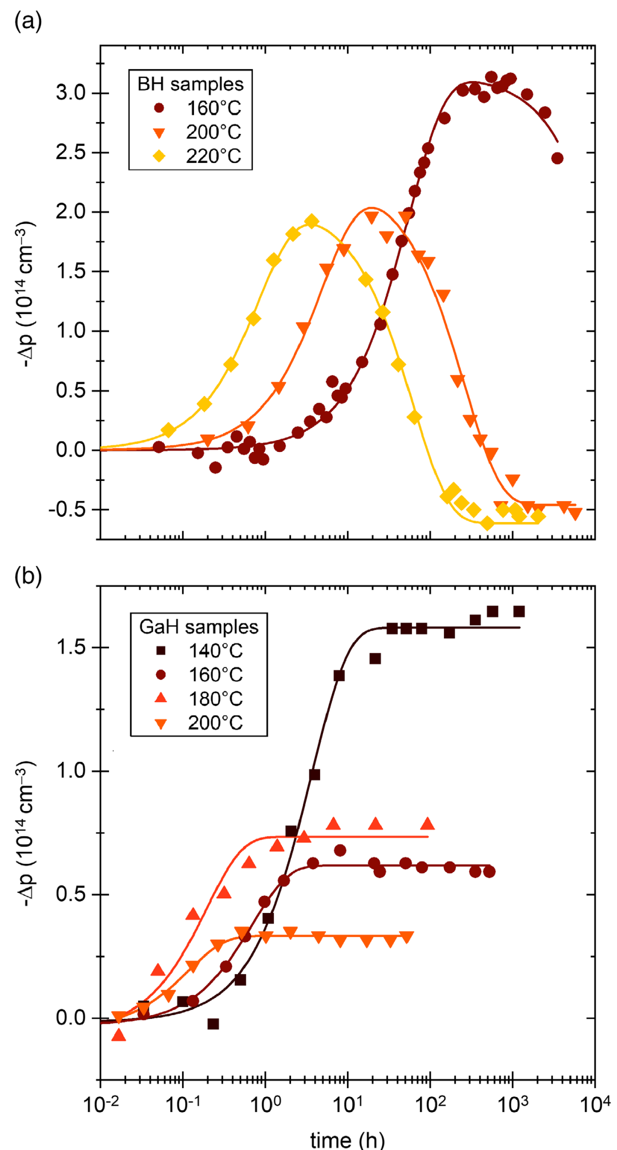

Figure 2. Change in (negative) hole concentration Δp with time relative to $t_0 = 0$ during annealing in the dark observed via resistance measurements for: a) the boron-doped samples and b) the gallium-doped samples.

required for the observed recovery of hole concentration. Assuming first-order reaction kinetics with constant reaction rates, which seems reasonable as $\Delta p \ll p$, the (change in) concentration of BH-pairs $[BH]$ should follow a double-exponential curve

$$[BH] = A_\infty - A_1 \times \exp(-R_1 \times t) + A_2 \times \exp(-R_2 \times t) \tag{2}$$

where R_1 and R_2 are effective reaction rates of the formation and dissociation reaction. As can be seen in Figure 2a, the double-exponential approach matches the measured data very well. As can be seen, as well, the data turn negative for long times indicating that some BH pairs already existed after sample preparation. Whether all BH pairs dissociate in the long run, i.e., $A_\infty = 0$, cannot be concluded from the shown data,

© 2022 The Authors. physica status solidi (a) applications and materials science published by Wiley-VCH GmbH

but FTIR measurements suggest a dissociation in large parts.[30] For the further analysis of reaction rates, this is not considered relevant.

3.2. Gallium–Hydrogen Dynamics

Unlike boron–hydrogen pairs, gallium–hydrogen pairs only seem to form and not to dissociate in the investigated temperature range and studied duration following the overall reaction

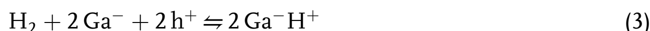

$$H_2 + 2\,Ga^- + 2\,h^+ \leftrightharpoons 2\,Ga^-H^+ \quad (3)$$

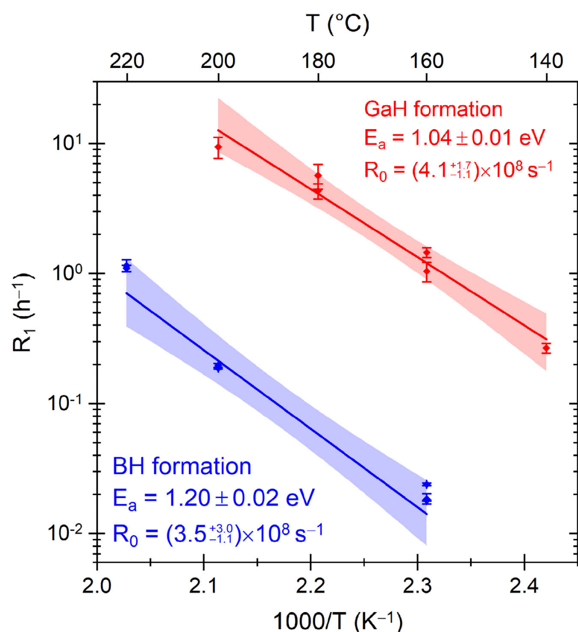

Figure 3. Effective reaction rates R_1 of BH and GaH pair formation in dependence of annealing temperature. The lines correspond to fits to the Arrhenius equation, the shaded area to a 95% confidence band.

Assuming again first-order reaction kinetics with constant reaction rates, the concentration of GaH pairs [GaH] should follow a single-exponentially rise-til-saturation curve

$$[\mathrm{GaH}] = A_\infty - A_1 \times \exp(-R_1 \times t) \quad (4)$$

The single-exponential approach fairly matches the data shown in Figure 2b. Note that the shown data do not allow any statement on already existent GaH pairs ($A_{\mathrm{inf}} - A_1$) and only reflect the change (A_1). Note as well that simulations suggest that the different extent of GaH pair formation is likely not related to a strengthened reverse reaction but more likely a consequence of different hydrogen concentrations in the samples. The suspected variation in hydrogen concentration is expected to impact observed reaction rates by not more than 10–20%.

3.3. Determination of Arrhenius Parameters

It is already obvious from the direct comparison of time scales of pair formation at the same temperature in Figure 2 that GaH pairs form faster than BH pairs. This can be seen more clearly in **Figure 3** where the reaction rates are shown in dependence on annealing temperature. To further quantify the individual behavior and clarify, whether this is due to a different effective activation energy E_a or due to a different trial frequency R_0 (i.e., attempts to create the pair per time), an analysis according to the Arrhenius equation

$$R(T) = R_0 \times \exp(-E_a/kT) \quad (5)$$

was done. Note that not the above equation is fitted to the reaction rates, but a linear regression is used on the logarithmic data, i.e., $\log(R)$. Even though it is maybe not that obvious from Figure 3, the effective activation energy of pair formation noticeably differs between BH pair formation (1.20 ± 0.02 eV) and GaH pair formation (1.04 ± 0.01 eV), but the trial frequency is almost the same ($3.5 \times 10^8\ s^{-1}$ vs $4.1 \times 10^8\ s^{-1}$).

To get a better impression of the significance of the results, a correlation analysis via a Monte Carlo approach was done to investigate the E_a–R_0-landscape in the vicinity of the best fit with

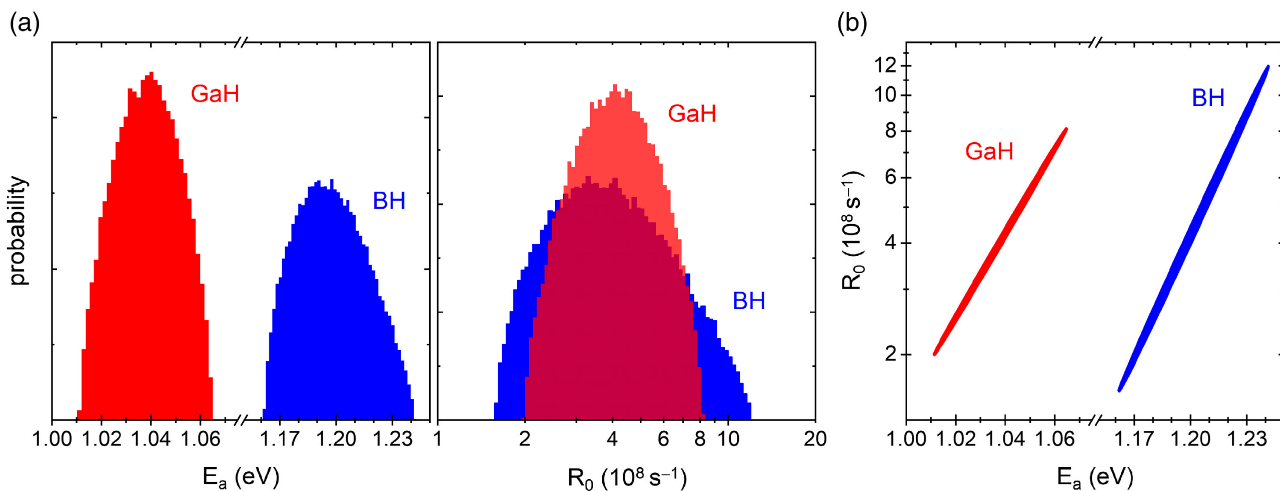

Figure 4. (left, middle) Probability distribution of activation energy E_a and trial frequency R_0 for the formation of BH and GaH pairs evaluated via a Monte Carlo approach. (right) Correlation diagram.

© 2022 The Authors. physica status solidi (a) applications and materials science published by Wiley-VCH GmbH

the lowest root-mean-square (RMS) value. Random deviations of the R_1 values obtained from Figure 1 (with Equation (2) or (4)) scaled with the individual uncertainties were chosen and the resulting data was fitted to obtain a probability distribution of E_a and R_0 with the RMS value exceeding the lowest one by only 1%. The findings are shown in **Figure 4**. As a result of linear regression, E_a follows (approx.) a normal distribution whereas trial frequency follows (approx.) a logarithmic normal distribution where median and mean differ systematically. Upon closer inspection, the probability distribution for the BH data deviates from the (logarithmic) normal distribution for both, E_a and R_0. In consequence, most probable, median (center) and mean value differ for the BH data set, even though the difference in R_0 is not too big ($3.5 \times 10^8\,s^{-1}$ vs $3.9 \times 10^8\,s^{-1}$ vs $4.4 \times 10^8\,s^{-1}$). We think that the most probable value is the most meaningful value and it is used for the line in Figure 3. The same accounts for E_a as well with the most probable value being 1.20 eV. There is a clear correlation of the fitted Arrhenius parameters where high activation energies coincide with high trial frequencies which is consistent with the expectation that a steeper curve features a higher y-axis interception.

4. Conclusion

The formation of boron–hydrogen (BH) and gallium–hydrogen (GaH) pairs in crystalline silicon from hydrogen dimers occurs on noticeably different time scales. The effective formation rate of GaH is in the investigated temperature range of 140 to 220 °C more than ten times higher than that for BH pairs. The Arrhenius analysis revealed that this is due to a difference in effective activation energy (1.04 eV vs 1.20 eV) but not due to a difference in trial frequency. The latter suggests that the mode of formation is comparable, but the energy barriers to overcome are different.

Acknowledgements

Part of this work was supported by the German Federal Ministry of Economic Affairs and Climate Action under contract number 03EE0152A. The content is the responsibility of the authors.

Open Access funding enabled and organized by Projekt DEAL.

Conflict of Interest

The authors declare no conflict of interest.

Data Availability Statement

The data that support the findings of this study are available from the corresponding author upon reasonable request.

Keywords

boron–hydrogen pairs, crystalline silicon, dynamics, gallium–hydrogen pairs

Received: March 1, 2022
Revised: May 24, 2022
Published online: July 9, 2022

[1] S. J. Pearton, J. W. Corbett, T. S. Shi, *Appl. Phys. A* **1987**, *43*, 153.
[2] B. Sopori, Y. Zhang, N. M. Ravindra, *J. Electron. Mater.* **2001**, *30*, 1616.
[3] S. Wilking, S. Ebert, A. Herguth, G. Hahn, *J. Appl. Phys.* **2013**, *114*, 194512.
[4] D. C. Walter, J. Schmidt, *Sol. Energy Mater. Sol. Cells* **2016**, *158*, 91.
[5] A. Herguth, B. Hallam, *AIP Conf. Proc.* **2018**, 130006.
[6] B. J. Hallam, P. G. Hamer, A. M. Ciesla née Wenham, C. E. Chan, B. V. Stefani, S. Wenham, *Progr. Photovolt. Res. Appl.* **2020**, *28*, 1217.
[7] M. A. Jensen, A. Zuschlag, S. Wieghold, D. Skorka, A. E. Morishige, G. Hahn, T. Buonassisi, *J. Appl. Phys.* **2018**, *124*, 085701.
[8] T. H. Fung, M. Kim, D. Chen, C. E. Chan, B. J. Hallam, R. Chen, D. N. Payne, A. Ciesla, S. R. Wenham, M. D. Abbott, *Sol. Energy Mater. Sol. Cells* **2018**, *184*, 48.
[9] J. Schmidt, D. Bredemeier, D. C. Walter, *IEEE J. Photovolt.* **2019**, *9*, 1497.
[10] D. Chen, P. Hamer, M. Kim, C. Chan, A. Ciesla nee Wenham, F. Rougieux, Y. Zhang, M. Abbott, B. Hallam, *Sol. Energy Mater. Sol. Cells* **2020**, *207*, 110353.
[11] C. Herring, N. M. Johnson, C. G. Van de Walle, *Phys. Rev. B* **2001**, *64*, 125209.
[12] C. G. Van De Walle, P. J. Denteneer, Y. Bar-Yam, S. T. Pantelides, *Phys. Rev. B* **1989**, *39*, 10791.
[13] C. Sun, F. E. Rougieux, D. Macdonald, *J. Appl. Phys.* **2015**, *117*, 045702.
[14] C. Sah, J. Y. Sun, J. J. Tzou, *Appl. Phys. Lett.* **1983**, *43*, 204.
[15] J. I. Pankove, R. O. Wance, J. E. Berkeyheiser, *Appl. Phys. Lett.* **1984**, *45*, 1100.
[16] W. L. Hansen, S. J. Pearton, E. E. Haller, *Appl. Phys. Lett.* **1984**, *44*, 606.
[17] M. J. Binns, S. A. McQuaid, R. C. Newman, E. C. Lightowlers, *Semicond. Sci. Technol.* **1993**, *8*, 1908.
[18] J. T. Borenstein, J. W. Corbett, S. J. Pearton, *J. Appl. Phys.* **1993**, *73*, 2751.
[19] R. E. Pritchard, J. H. Tucker, R. C. Newman, E. C. Lightowlers, *Semicond. Sci. Technol.* **1999**, *14*, 77.
[20] V. V. Voronkov, R. Falster, *Phys. Status Solidi B* **2017**, *254*, 1600779.
[21] A. J. Tavendale, D. Alexiev, A. A. Williams, *Appl. Phys. Lett.* **1985**, *47*, 316.
[22] C. H. Seager, R. A. Anderson, *Appl. Phys. Lett.* **1988**, *53*, 1181.
[23] T. Zundel, A. Mesli, J. C. Muller, P. Siffert, *Appl. Phys. A Solids Surf.* **1989**, *48*, 31.
[24] D. C. Walter, D. Bredemeier, R. Falster, V. V. Voronkov, J. Schmidt, *Sol. Energy Mater. Sol. Cells* **2019**, *200*, 109970.
[25] A. Herguth, C. Winter, *IEEE J. Photovolt.* **2021**, *11*, 1059.
[26] M. Sheoran, D. S. Kim, A. Rohatgi, H. F. Dekkers, G. Beaucarne, M. Young, S. Asher, *Appl. Phys. Lett.* **2008**, *92*, 172107.
[27] C. Winter, J. Simon, A. Herguth, *Phys. Status Solidi A* **2021**, 2100220.
[28] E. Schneiderlöchner, R. Preu, R. Lüdemann, S. W. Glunz, *Progr. Photovolt. Res. Appl.* **2002**, *10*, 29.
[29] PV Lighthouse, Mobility Calculator, https://www2.pvlighthouse.com.au/calculators/mobility%20calculator/mobility%20calculator.aspx (accessed: April 2021).
[30] J. Simon, A. Herguth, G. Hahn, *J. Appl. Phys.* **2022**, *131*, 235703.

© 2022 The Authors. physica status solidi (a) applications and materials science published by Wiley-VCH GmbH